

# Macroscopic descriptions of follower-leader systems

S. Bernardi<sup>1</sup>, G. Estrada-Rodriguez<sup>2</sup>, H. Gimperlein<sup>2,3</sup> and K. J. Painter<sup>2</sup>

<sup>1</sup> *Dipartimento di Scienze Matematiche, Politecnico di Torino, Corso Duca degli Abruzzi 24, 10129 Torino, Italy*  
*email: s.bernardi@unito.it*

<sup>2</sup> *Maxwell Institute for Mathematical Sciences and Department of Mathematics, Heriot-Watt University, Edinburgh, EH14 4AS, United Kingdom*  
*email: {ge5, h.gimperlein, k.painter}@hw.ac.uk*

<sup>3</sup> *Institute for Mathematics, University of Paderborn, Warburger Str. 100, 33098 Paderborn, Germany*

The fundamental derivation of macroscopic model equations to describe swarms based on microscopic movement laws and mathematical analyses into their self-organisation capabilities remains a challenge from both modelling and analysis perspectives. In this paper we clarify relevant continuous macroscopic model equations that describe follower-leader interactions for a swarm where these two populations are fixed, using the case example of honeybee swarming to motivate our model. We study the behaviour of the swarm over long and short time scales to shed light on the number of leaders needed to initiate swarm movement, according to the homogeneous or inhomogeneous nature of the interaction (alignment) kernel. The results indicate the crucial role played by the interaction kernel to model transient behaviour.

**Key Words:** Follower-leader systems, interacting particle systems, velocity-jump model, macroscopic limit, swarming, bees.

**2010 Mathematics Subject Classification:** 92D25 (Primary); 92D50; 35Q92; 82C22 (Secondary)

---

## 1 Introduction

Collective movements describe the tendency of a group of individuals to coordinate their motion in a manner that generates net flow of the entire population. Examples range from cells to animals, from migrating cell clusters during development and cancer invasion [22, 28] to shifting bird flocks and fish shoals; the latter extend to the kilometre-spanning shoals formed from hundreds of millions of herrings [27]. A point of recent interest concerns the potential division of a population into “leaders” and “followers” and, consequently, how leaders influence swarm dynamics. Clearcut leadership could result from experience, age or prior knowledge: the presence of older birds improves path efficiency in migrating cranes [30]; post-menopausal orcas adopt leading positions during

pod foraging [7]; only the “househunting” scouts know the final destination of a new honeybee nest [38]. Subtler leaders arise within superficially identical populations, such as the presence of faster or “braver” individuals in fish shoals and bird flocks [35, 31]. Leader/follower statuses also occur in a host of cellular systems, ranging from collective movements of aggregated amoebae to sprouting blood capillaries during development, physiology and disease [28].

Most theoretical descriptions of collective migration have employed agent/particle-based approaches, e.g. [44, 10, 9, 12, 11], see also [3]. Despite the plethora of models, they typically share a so-called set of “first principles of swarming” [8]: specifically, particle trajectories governed by a combination of repulsion (preventing collisions), attraction/cohesion (preventing dispersal) and alignment of direction/velocity according to neighbour positions, each operating over specified interaction ranges. Models based on these features reproduce a wide variety of collective migration phenomenologies, e.g. see [3]. In the context of follower-leader systems, a key finding has been that swarms can be efficiently guided by a small number of anonymous (i.e. not clearly distinct from the crowd) informed individuals [9]. These individuals influence their neighbours, which in turn influence further followers and knowledge is relayed through the swarm. Surprisingly, as the swarm population increases a diminishing fraction of leaders is needed to achieve the same level of guidance efficiency [9]. Follower-leader alignment strategies have also been incorporated within other swarming studies. For example, in [23] a “transient leadership” model was considered to imitate bird flocks while “hierarchical leadership” was studied in [41] within the framework of a Cucker-Smale model.

Beyond agent-based models, a plethora of continuous models have been proposed, for example see [29, 43, 17, 18, 33]. In common with their individual-based counterparts, movement is governed by a set or subset of attracting/repelling/aligning interactions, typically generating integro-differential equations of parabolic (e.g. [29, 33]) or hyperbolic (e.g. [18]) form. While these models gain analytical tractability, their connection to individual-level behaviour is inevitably blurred.

In this paper we derive macroscopic partial differential equations (PDEs) to describe follower-leader interactions within swarming populations, starting from an underlying particle description for movement. In particular, we exploit the well-studied exemplar of honeybee swarming to frame our modelling assumptions. In the next section we summarise key properties and prior modelling in this system, subsequently refining to a relatively minimal set of assumptions to test whether a simple process of velocity alignment can generate coherent and guided swarm movement. We proceed to examine hyperbolic and parabolic scaling limits under homogeneous and inhomogeneous interaction (alignment) kernels and discuss the new modelling challenges to describe realistic follower-leader dynamics.

## 2 Honeybee swarming

### 2.1 Biological background

When a colony of honeybees outgrows its home, two-thirds of the population (including the queen) departs. While the remaining population raises a new queen and forms a

daughter colony, the homeless bees bivouac nearby while scouts scour the countryside for a new site. Reappearances at the colony are accompanied by a “waggle dance”, communicating distance, direction and quality of possible new nests to other scouts. Proposals are analysed before consensus is achieved, at which point the population takes to the air and the scouts guide the ensuing swarm to the new nest, potentially several kilometres away [38]. Given that only a small (3%-5%) proportion of the swarm are scouts, successful translocation relies on the ability of a small percentage of informed individuals – from a few hundred to a thousand for the 10,000+ swarm [40, 39] – to impart their knowledge.

Early observations of “high-speed” bees, flying in the upper portion of the swarm and towards the nest site, led to the suggestion that this population coincided with the scouts and that the behaviour allowed followers to infer nest direction [26]. Subsequent studies have tested this “streaker hypothesis” against alternative theories of swarm guidance [40, 1, 37, 21]. For example, thorough analysis of individual trajectories in videoed swarms supports the presence of streakers, along with their localisation towards the upper swarm [1, 37]. Harmonic radars applied to scouts prior to the swarm’s movement revealed a subsequent streaker-like behaviour, with fast bursts of nest-directed movements interspersed with periods of negligible or slower movements in the opposite direction [21]. A fast-flying line of foragers across a swarm’s path disrupts swarm guidance, consistent with the theory that fast-flying behaviour impacts on a bee’s flight trajectory [25].

Inevitably, streaking sends scouts to the leading swarm edge, so questions arise on their subsequent behaviour. Two proposals, suggested in [38], are: (i) slowly travelling backwards, perhaps along the bottom or sides to minimise their influence, or (ii) “waiting out” the swarm’s passage, before rejoining and streaking again. Harmonic radar experiments provide some support for either mechanism [21], though technical limitations are unable to give precise answers at present. Questions also arise on just how much guidance information is transmitted from streakers to uninformed bees. Flying fast at the top clearly raises visibility, but despite growing understanding of their visual abilities (e.g. [36]), the extent, range and manner of bee alignment to their conspecifics remains unclear. Do followers synchronise movements to all their near neighbours or just the fastest? Over what range can streaker bees be identified? In short, what is the extra weighting generated through performing a streak?

## 2.2 Prior modelling

Among numerous models of collective movement, several have specifically focussed on bee swarms. For example, Fetecau and Guo [20] implement a first-order model involving attraction, repulsion (described by a Morse potential) and alignment, along with a random component activated only under low interactions between an individual and the rest of the swarm. Each bee’s visual field corresponds to a planar cone aligned in their direction of motion and formed from two regions: individuals in a central cone are fully seen, while those in the peripheral region are partially seen (and ascribed lower weight). Further, a leader subpopulation ignores other swarm members and moves in oscillatory fashion, with fast/high-visibility movements towards the nest until they reach the front edge, followed by slower/low-visibility movements towards the rear. Attraction, repul-

sion and alignment also lie at the heart of a first-order model in [24]. Alignment follows a Euclidean metric-based assumption, with (follower) bees synchronising their movements according to all visible neighbours, regardless of their speed. As in [20], a set of leaders is given a back-and-forth motion.

The model in [16] incorporates both site decision-making and subsequent swarm guidance. Regarding the latter, a cohesion term attracts each bee according to the barycenter of a set of sufficiently fast individuals, along with their topological metric-based alignment. The resulting model was applied to compare swarming of two honeybee species, *Apis mellifera* and *Apis florea*. The same basic rules are implemented in [5] to study whether a single leader can transmit guidance to an entire swarm, testing both topological (a fixed number of bees, regardless of distance) and metric-based (all bees within a set region) alignments. Efficient guidance occurred for either a sufficiently large region (encompassing the entire bee cloud) under metric alignment or for a high enough number of groupmates (i.e.  $\geq 13$ ) under topological alignment. Extensions in [6] considered how the subtlety of scout visibility and behaviour impacted on swarm efficiency. Further, the scout percentage to total swarm size relationship was addressed, with larger swarms demanding a smaller fraction of scouts to achieve comparable targeting, echoing the results of earlier models [9, 20]. Further additions included greater environmental complexity, e.g. forcing swarms to circumnavigate structural elements. Finally, in [4] models were tested against experiments on swarm disruption due to high velocity forager highways [25]. Based on fitting against data, the leading plausible set of model assumptions involved follower bees synchronising movement according to all sufficiently close insects (regardless of their status), provided that passive leaders slowly returned from the front to the rear edge of the swarm.

### 3 Swarm description

We assume the swarm is divided into two main subpopulations: followers ( $f$ ) and leaders, with the latter further subdivided into those engaging as streakers ( $s$ ) and those behaving passively ( $p$ ). The total number of leaders is considered small (for bees, 3% – 5% of the total population e.g. [38]) compared to the followers. We assume that the leaders have knowledge of the nest location while the followers are completely uninformed. Streakers correspond to those leaders flying fast in the nest direction, while passive leaders are those behaving otherwise. Specifically, we assume that (i) a streaker flies fast to the swarm's front edge, (ii) switches to a passive role and returns more slowly towards the rear, and (iii) closes the cycle by switching back to a streaker role. Streaking is marked by the distinctive velocity, so that streakers lead the swarm through flying with fixed maximum speed  $c_s$  in the direction of the nest and alerting followers of the nest direction in the process. Followers and passive leaders, meanwhile, are presumed to fly with fixed speeds  $c_f$  and  $c_p$  respectively.

An obviously important quantity in the model is the position of the swarm with respect to the nest. Given a generic bee located at  $\mathbf{x}_k$ , its distance to the nest at  $\mathbf{x}_{\text{nest}}$  is denoted by  $I_{\text{nest}}(\mathbf{x}_k(t)) = |\mathbf{x}_k(t) - \mathbf{x}_{\text{nest}}|$ . We fix a corresponding field  $\mathbf{b} \simeq \nabla I_{\text{nest}}$  within the domain outside the nest, such that  $-\mathbf{b}$  defines the direction for the leaders to the nest.

Specifically, we choose  $\mathbf{b} = \nabla I_{\text{nest}}$  to be divergence free at the nest and tangent to the boundary of the domain. As  $|\mathbf{x}| \rightarrow \infty$ , we impose  $\mathbf{b}(\mathbf{x}) \rightarrow \nabla I_{\text{nest}}$ .

We define  $\bar{\sigma}_i(\mathbf{x}, t, \theta, \tau)$ , for  $i \in \{f, p, s\}$ , as the *microscopic densities* of followers, passive leaders and streakers at position  $\mathbf{x}$ , time  $t$ , moving in direction  $\theta$  for some time  $\tau$ . Integrating with respect to  $\tau$ , we denote  $\sigma_i(\mathbf{x}, t, \theta) = \int_0^t \bar{\sigma}_i(\mathbf{x}, t, \theta, \tau) d\tau$  as the density of each subpopulation at position  $\mathbf{x}$ , time  $t$  and moving in direction  $\theta$ . Subsequently integrating over  $\theta$  generates the *macroscopic densities*

$$\rho_i(\mathbf{x}, t) = \frac{1}{|S|} \int_0^t \int_S \bar{\sigma}_i(\cdot, \theta, \tau) d\theta d\tau,$$

where  $S = \{\mathbf{x} \in \mathbb{R}^n : |\mathbf{x}| = 1\}$  is the unit sphere in  $\mathbb{R}^n$  with surface area  $|S|$ . Dropped subscripts are used to denote total population densities, i.e.  $\bar{\sigma} = \bar{\sigma}_f + \bar{\sigma}_p + \bar{\sigma}_s$ ,  $\sigma = \sigma_f + \sigma_p + \sigma_s$  and  $\rho = \rho_f + \rho_p + \rho_s$ .

The dynamics of each subpopulation are described according to a set of rules, minimally chosen to sufficiently describe swarm behaviour while restricting excess complexity. For the followers we assume:

- 1F. Trajectories comprise of straight line motions interrupted by (effectively) instantaneous reorientations, where the new direction of motion is randomly chosen. This movement is called a velocity-jump process [32]. Individuals stop (i.e. reorient) with a rate given by a fixed parameter  $\beta$ .
- 2F. At each reorientation, with probability  $\zeta \in (0, 1)$  it selects a new direction of motion  $\eta$ , taken to be symmetrically distributed with respect to the previous one according to

$$k(\mathbf{x}, t, \theta; \eta) = \tilde{k}(\mathbf{x}, t, |\eta - \theta|).$$

Because  $\tilde{k}$  is a probability distribution, it is normalized to  $\int_S \tilde{k}(\mathbf{x}, t, |\theta - e_1|) d\theta = 1$  where  $e_1 = (1, 0, \dots, 0)$ . The turn angle operator  $T$  is defined as

$$T\phi(\eta) = \int_S k(\mathbf{x}, t, \theta; \eta) \phi(\theta) d\theta. \quad (3.1)$$

Trivially,  $\tilde{k}$  could be a uniform distribution; more generally, a bias according to the previous orientation would incorporate an element of persistence of orientation, so we consider  $\tilde{k}(|\eta - \theta|)$ .

- 3F. With probability  $1 - \zeta$  the follower instead aligns with the orientation of the local population, according to

$$\Lambda(\mathbf{x}, \theta, t) = \frac{\mathcal{J}(\mathbf{x}, t)}{|\mathcal{J}(\mathbf{x}, t)|}, \quad \mathcal{J}(\mathbf{x}, t) = \int_{\mathbb{R}^n} \int_S K(|\mathbf{y} - \mathbf{x}|) \sigma(\mathbf{y}, t, \theta) \theta d\mathbf{y} d\theta. \quad (3.2)$$

If the flux  $\mathcal{J}(\mathbf{x}, t) = 0$ , we assume that  $\Lambda(\mathbf{x}, \theta, t)$  takes the value  $\theta$  [14]. A slight generalisation of the above would be to choose something of the form:

$$\Lambda(\mathbf{x}, \theta, t) = \frac{\mathcal{J}(\mathbf{x}, t)}{|\mathcal{J}(\mathbf{x}, t)|}, \quad \mathcal{J}(\mathbf{x}, t) = \int_{\mathbb{R}^n} \int_S K(|\mathbf{y} - \mathbf{x}|) (\sigma_f + \sigma_p + \lambda \sigma_s) d\mathbf{y} d\theta. \quad (3.3)$$

where  $\lambda \geq 1$  would reflect that streakers have higher visibility and therefore provide greater weighting to the orientation of the followers. We note that the limitations of

the above homogeneous choice will be discussed in Section 4.3. In particular, an inhomogeneous variant, given by  $\Lambda(\mathbf{x}, t) = \nu \mathcal{J}(\mathbf{x}, t)$ , will subsequently be considered in Section 5.

4F.  $c_f \lesssim c_s$ .

Rules for the passive leaders are given by:

- 1P. They also move according to a velocity jump process as described in 1F, with the same stopping rate  $\beta$ .
- 2P. No alignment according to other individuals.
- 3P. Passive leaders move in the direction of the rear of the swarm (effectively, in the direction of  $\mathbf{b}$ ).
- 4P. The new direction of motion  $\eta$  is then biased by these two quantities and is given by the turn angle operator

$$B(\mathbf{x}, \eta) = B^0(\eta) + B^1(\mathbf{x}, \eta) = T + T_{\rho_f} .$$

To be specific, we fix  $T_{\rho_f} = (\mathbf{b} \cdot \nabla \rho_f) \nabla \rho_f$ . Note that this operator does not depend on the incoming direction.

5P.  $c_p \lesssim c_s$ .

- 6P. Transitions between streaker and passive leader take place at the front and rear edges of the swarm, as described below.

Finally, streakers move according to:

- 1S. Given their knowledge of their nest, they move as ballistic particles in direction  $-\mathbf{b}$  (towards the front of the swarm as represented in Figure 1), with a fixed maximum speed given by  $c_s$ . Thus, no randomness is assumed.
- 2S. Transitions between streaker and passive leader take place at the front and rear edges of the swarm, as described below.

We note that as movements into orientations outside  $-\mathbf{b}$  are not permitted for leaders within this model, evolution equations for the streakers will be written directly at the level of the macroscopic density  $\rho_s$ . Microscopic densities can then be inferred as singular distributions, where the local macroscopic density is concentrated into orientation  $-\mathbf{b}$ : i.e.,  $\sigma_s(\mathbf{x}, t, \theta) = \rho_s(\mathbf{x}, t) \delta(\theta + \mathbf{b})$  where  $\delta$  is the Dirac delta function.

Suppose a Gaussian-type curve for the swarm profile. Physically, the transition rate from streaker to passive leader,  $R_{sp}$ , should be localised to the front edge of a swarm: in a region where  $(\nabla \rho_f, \mathbf{b}) > 0$ , as illustrated in Figure 1. As follower densities decrease, i.e.  $\rho_f \rightarrow 0$ ,  $R_{sp}$  should be bounded away from zero:  $R_{sp} \geq r_0 > 0$  as  $\rho_f \rightarrow 0$ , where  $r_0$  is the minimal conversion rate outside the swarm. The rules for transition rate from passive leaders to streakers,  $R_{ps}$ , obey similar rules. Transitions should be concentrated to the rear edge of the swarm, i.e. where  $(\nabla \rho_f, \mathbf{b}) < 0$ . Again, as follower densities decrease we require  $R_{ps} \geq r_0 > 0$ .

For more complicated swarm profiles, e.g. dual peaked as in Figure 2, let  $c_s/r_0$  define a length scale on which the density of streakers (and hence also that of passive leaders) varies. If the spacing between the two peaks is sufficiently larger than  $c_s/r_0$  then streakers

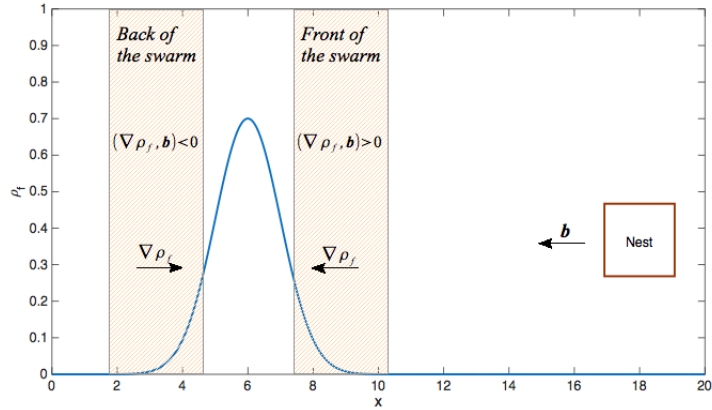


Figure 1. Illustration of switching between streakers and passive leaders.

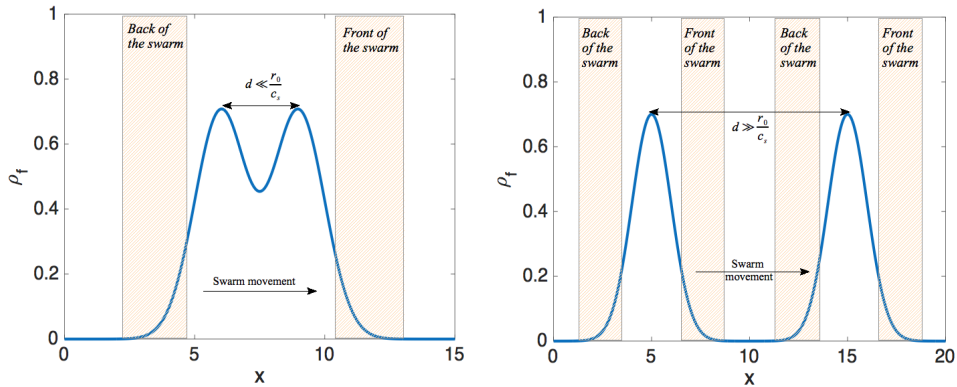


Figure 2. Illustration of different swarm shapes.

consider the blobs as separate swarms and there are separate fronts and backs for each swarm. For peaks spaced below this distance, the majority of streakers fly towards the leading edge before converting to passive leaders and it can be considered a single swarm with a single leader population.

We note that while a change from passive to streaker leader involves transition into a population with fixed orientation, a streaker to passive change demands transition into a population distributed over the unit sphere. We define  $R_{sp} = \frac{1}{|S|} \int_S R_{sp}(\theta) d\theta$ .

### 3.1 Microscopic description

Following the swarm description given in Section 3, the population densities satisfy systems of integro-differential equations as follows. For the streakers and passive leaders,

$$\partial_t \rho_s - c_s \mathbf{b} \cdot \nabla \rho_s = -R_{sp} \rho_s + R_{ps} \rho_p, \quad (3.4)$$

$$\left\{ \begin{array}{l} (\partial_\tau + \partial_t + c_p \theta \cdot \nabla) \bar{\sigma}_p(\cdot, \theta, \tau) - R_{sp}(\theta) \rho_s + R_{ps} \bar{\sigma}_p(\cdot, \theta, \tau) = -\beta \bar{\sigma}_p(\cdot, \theta, \tau), \\ \bar{\sigma}_p(\cdot, \eta, \tau = 0) = \int_0^t \int_S B(\mathbf{x}, \eta) \beta \bar{\sigma}_p(\cdot, \theta, \tau) d\theta d\tau . \end{array} \right. \quad (3.5)$$

For the followers, following the approach in [19], we have

$$\left\{ \begin{array}{l} (\partial_\tau + \partial_t + c_f \theta \cdot \nabla) \bar{\sigma}_f(\cdot, \theta, \tau) = -\beta \bar{\sigma}_f(\cdot, \theta, \tau) , \\ \bar{\sigma}_f(\cdot, \eta, \tau = 0) = \int_S Q(\eta, \theta) \int_0^t \beta \bar{\sigma}_f(\cdot, \theta, \tau) d\tau d\theta , \end{array} \right. \quad (3.7)$$

where

$$Q(\eta, \theta) = \zeta \tilde{k}(|\eta - \theta|) + (1 - \zeta) \Phi(\Lambda \cdot \eta) . \quad (3.9)$$

$\Phi(\Lambda \cdot \eta)$  is the distribution of the new aligned direction and satisfies  $\int_S \Phi(\Lambda \cdot \eta) d\eta = 1$ . Integrating with respect to  $\tau$  the system (3.5)-(3.6) we obtain, for  $\sigma_p(\cdot, \theta) = \int_0^t \bar{\sigma}_p(\cdot, \theta, \tau) d\tau$ ,

$$\begin{aligned} \partial_t \sigma_p + c_p \theta \cdot \nabla \sigma_p - R_{sp}(\theta) \rho_s + R_{ps} \sigma_p &= -\beta \sigma_p + \bar{\sigma}_p(\cdot, \theta, 0) \\ &= -\beta \sigma_p + B(\mathbf{x}, \theta) \beta \int_0^t \int_S \bar{\sigma}_p(\cdot, \eta, \tau) d\eta d\tau . \end{aligned} \quad (3.10)$$

Defining the macroscopic density  $\rho_p(\mathbf{x}, t) = \frac{1}{|S|} \int_0^t \int_S \bar{\sigma}_p(\cdot, \eta, \tau) d\eta d\tau$ , we obtain the mesoscopic equation

$$\partial_t \sigma_p + c_p \theta \cdot \nabla \sigma_p = R_{sp}(\theta) \rho_s - R_{ps} \sigma_p - \beta \sigma_p + |S| \beta B \rho_p . \quad (3.11)$$

Similarly, integrating system (3.7)-(3.8) with respect to  $\tau$  and using the definition of  $T$  given in (3.1) we obtain

$$\partial_t \sigma_f + c_f \theta \cdot \nabla \sigma_f = -\beta \sigma_f + \zeta \beta T \sigma_f + (1 - \zeta) \beta \Phi(\Lambda \cdot \theta) \rho_f . \quad (3.12)$$

#### 4 Macroscopic PDE description

As shown in the previous section, the densities  $\rho_s(\mathbf{x}, t)$ ,  $\sigma_p(\mathbf{x}, t, \theta)$  and  $\sigma_f(\mathbf{x}, t, \theta)$  satisfy the following system of kinetic equations,

$$\partial_t \rho_s - c_s \mathbf{b} \cdot \nabla \rho_s = -R_{sp} \rho_s + R_{ps} \rho_p , \quad (4.1)$$

$$\partial_t \sigma_p + c_p \theta \cdot \nabla \sigma_p = R_{sp}(\theta) \rho_s - R_{ps} \sigma_p - \beta \sigma_p + |S| \beta B \rho_p , \quad (4.2)$$

$$\partial_t \sigma_f + c_f \theta \cdot \nabla \sigma_f = -\beta \sigma_f + \zeta \beta T \sigma_f + (1 - \zeta) \beta \Phi(\Lambda \cdot \theta) \rho_f . \quad (4.3)$$

Treating the population of streakers and passive leaders as the total population of leaders,  $\rho_\ell = \rho_s + \rho_p$ , we derive a conservation equation for  $\rho_\ell$ .

First, integrating (4.2) with respect to  $\theta$  we obtain

$$\partial_t \rho_p + n c_p \nabla \cdot w_p = R_{sp} \rho_s - R_{ps} \rho_p , \quad (4.4)$$

where

$$\rho_p = \frac{1}{|S|} \int_S \sigma_p d\theta \quad \text{and} \quad w_p = \frac{1}{n|S|} \int_S \theta \sigma_p d\theta , \quad (4.5)$$

and where we assumed that the turn angle operator  $B$  preserves the number of particles, i.e.,  $\int_S B d\theta = 1$ . Adding the resulting equation (4.4) together with (4.1) we obtain

$$\partial_t \rho_\ell + n c_p \nabla \cdot w_p - c_s \nabla \cdot (\mathbf{b} \rho_s) = 0 , \quad (4.6)$$

where  $\nabla \cdot (\mathbf{b} \rho_s) = \mathbf{b} \cdot \nabla \rho_s$ , provided that  $\nabla \cdot \mathbf{b} = 0$  as follows from the definition of  $\mathbf{b}$  in Section 3.

Similarly, we control that the population of the followers (4.3) is conserved:

$$\partial_t \int_S \sigma_f d\theta + c_f \int_S \theta \cdot \nabla \sigma_f d\theta = -\beta \int_S \sigma_f d\theta + \zeta \beta \int_S T \sigma_f d\theta + (1 - \zeta) \beta \rho_f = 0 , \quad (4.7)$$

since  $\int_S \Phi(\Lambda \cdot \theta) d\theta = 1$  and  $\int_S T d\theta = 1$  by definition.

#### 4.1 Diffusion limit

Next we turn to determining macroscopic equations that describe the interactions between the three different populations over long time regimes. Introducing a parabolic scaling  $(\mathbf{x}, t) \mapsto (\mathbf{x}/\varepsilon, t/\varepsilon^2)$ , transition rates  $R_{sp}^\varepsilon, R_{ps}^\varepsilon$  are multiplied by a factor of  $\varepsilon$  and  $T_{\rho_f}^\varepsilon = \varepsilon^2 (\mathbf{b} \cdot \nabla \rho_f) \nabla \rho_f$ . The operator  $B^\varepsilon(\mathbf{x}, \theta)$  satisfies  $\int_S B^\varepsilon(\mathbf{x}, \theta) \theta d\theta = \varepsilon C(\nabla \rho_f) \nabla \rho_f$  to leading order in  $\varepsilon$ .

Equations (4.1), (4.2) and (4.3) then become

$$\varepsilon^2 \partial_t \rho_s - \varepsilon c_s \mathbf{b} \cdot \nabla \rho_s = -\varepsilon R_{sp}^\varepsilon \rho_s + \varepsilon R_{ps}^\varepsilon \rho_p , \quad (4.8)$$

$$\varepsilon^2 \partial_t \sigma_p + \varepsilon c_p \theta \cdot \nabla \sigma_p = \varepsilon R_{sp}^\varepsilon(\theta) \rho_s - \varepsilon R_{ps}^\varepsilon \sigma_p - \beta \sigma_p + |S| \beta B^\varepsilon \rho_p , \quad (4.9)$$

$$\varepsilon^2 \partial_t \sigma_f + \varepsilon c_f \theta \cdot \nabla \sigma_f = -\beta \sigma_f + \zeta \beta T \sigma_f + (1 - \zeta) \beta \Phi^\varepsilon(\Lambda \cdot \theta) \rho_f . \quad (4.10)$$

Let us suppose that the total population of passive leaders,  $\sigma_p$ , can be written in terms of the following expansion:

$$\sigma_p = \sigma_p^0 + \varepsilon \sigma_p^1 + \mathcal{O}(\varepsilon^2) . \quad (4.11)$$

Substituting the above expression into (4.9) and letting  $\varepsilon \rightarrow 0$ ,

$$\varepsilon^0 : \quad \sigma_p^0 = |S| B^0 \rho_p , \quad (4.12)$$

$$\varepsilon^1 : \quad \sigma_p^1 = \frac{1}{\beta} (-c_p \theta \cdot \nabla \sigma_p^0 + R_{sp}^0(\theta) \rho_s - R_{ps}^0 \sigma_p^0) . \quad (4.13)$$

We obtain a Chapman-Enskog expansion from (4.11):

$$\sigma_p = |S| B^0 \rho_p + \varepsilon \sigma_p^1 + \mathcal{O}(\varepsilon^2) . \quad (4.14)$$

Substituting the above expression into the mean direction of the passive leaders,  $w_p$  in (4.5), we obtain

$$\begin{aligned} w_p &= \frac{1}{n} \int_S \theta B^0(\theta) d\theta \rho_p + \frac{\varepsilon}{n|S|} \int_S \theta \sigma_p^1 d\theta , \\ &= \frac{1}{n} \mathcal{B}_\theta^0 \rho_p + \frac{\varepsilon}{n|S|} \int_S \theta \sigma_p^1 d\theta , \end{aligned}$$

where  $\mathcal{B}_\theta^0 = \int_S \theta B^0 d\theta$ . The conservation equation for the leaders (4.6), is then

$$\varepsilon^2 \partial_t \rho_\ell + \varepsilon c_p \nabla \cdot \left( \mathcal{B}_\theta^0 \rho_p + \frac{\varepsilon}{|S|} \int_S \theta \sigma_p^1 d\theta \right) - \varepsilon c_s \nabla \cdot (\mathbf{b} \rho_s) = 0 . \quad (4.15)$$

The term  $\nabla \cdot \int_S \theta \sigma_p^1 d\theta$  can be explicitly computed using (4.12) and (4.13) as follows:

$$\begin{aligned} \frac{1}{|S|} \nabla \cdot \int_S \theta \sigma_p^1 d\theta &= \frac{-c_p}{|S|\beta} \int_S (\nabla \cdot \theta)(\theta \cdot \nabla) B^0 \rho_p d\theta + \frac{1}{|S|} \nabla \cdot \int_S \theta \left( R_{sp}^\varepsilon(\theta) \rho_s + |S| R_{ps}^\varepsilon B^0 \rho_p \right) d\theta , \\ &= -\Delta(D\rho_p) + \nabla \cdot (R_{sp}^\varepsilon(\theta) \rho_s) + R_{ps}^\varepsilon \nabla \cdot (B_\theta^0 \rho_p) , \end{aligned}$$

where

$$D = \frac{c_p}{|S|\beta} \int_S \theta \theta^T B^0 d\theta \quad \text{and} \quad R_{sp}^\varepsilon(\theta) = \frac{1}{|S|} \int_S \theta R_{sp}^\varepsilon(\theta) d\theta .$$

$D$  is the diffusion coefficient and  $R_{sp}^\varepsilon$  describes some turning of the streaker population  $\rho_s$ .

If we substitute  $\rho_\ell = \rho_s + \rho_p$  into the scaled conservation equation (4.15) and  $\partial_t \rho_s$  from (4.8), we observe that as  $\varepsilon \rightarrow 0$  we obtain from the leading order  $c_p \nabla \cdot (B_\theta^0 \rho_p) = R_{sp}^0 \rho_s - R_{ps}^0 \rho_p$ . Finally, for the passive leaders we have

$$\partial_t \rho_p - nc_p \Delta(D\rho_p) + nc_p \nabla \cdot (R_{sp}^0 \rho_s) + nc_p R_{ps}^0 \nabla \cdot (B_\theta^0 \rho_p) = 0 . \quad (4.16)$$

The conservation equation (4.7) for the follower population is

$$\partial_t \rho_f + nc_f \nabla \cdot w_f = 0 , \quad (4.17)$$

where  $w_f = \frac{1}{n\varepsilon|S|} \int_S \theta \sigma_f d\theta$ . To compute the mean direction of the followers,  $w_f$ , we multiply (4.10) by  $\theta$  and integrate over  $S$ ,

$$\begin{aligned} \varepsilon^2 \int_S \theta \sigma_f d\theta + \varepsilon c_f \nabla \int_S \theta \theta^T \sigma_f d\theta &= -\beta \int_S \theta \sigma_f d\theta + \zeta \beta \int_S \theta T \sigma_f d\theta \\ &\quad + (1 - \zeta) \beta \rho_f \int_S \theta \Phi^\varepsilon(\Lambda \cdot \theta) d\theta . \end{aligned} \quad (4.18)$$

Using the expansion  $\sigma_f = |S|^{-1}(\rho_f + \varepsilon n \theta \cdot w_f)$  and letting  $\varepsilon \rightarrow 0$  we obtain

$$w_f = \frac{1 - \zeta}{n(1 - \zeta \nu_1)} \rho_f \int_S \theta \Phi^0(\Lambda^W \cdot \theta) d\theta - \frac{c_f}{n\beta(1 - \zeta \nu_1)} \nabla \rho_f , \quad (4.19)$$

where  $\Phi^0(\Lambda^W \cdot \theta) = \lim_{\varepsilon \rightarrow 0} \Phi^\varepsilon(\Lambda^W \cdot \theta)$ ,  $W$  is the total mean direction of the whole population and

$$\Lambda^W = \frac{\mathcal{J}^W}{|\mathcal{J}^W|} \quad \text{for} \quad \mathcal{J}^W = \frac{n\varepsilon}{|S|} \int_{\mathbf{y}} K^\varepsilon \left( \frac{|\mathbf{y} - \mathbf{x}|}{\varepsilon} \right) W(\mathbf{y}, t) d\mathbf{y} .$$

If we consider  $\mathcal{J}$  as in (3.3) then the mean direction,  $\Lambda$ , will depend only on the mean direction of the streakers,  $w_s$ , as follows

$$\Lambda^s = \frac{\mathcal{J}^s}{|\mathcal{J}^s|} \quad \text{where} \quad \mathcal{J}^s = \frac{n\varepsilon\lambda}{|S|} \int_{\mathbf{y}} K^\varepsilon \left( \frac{|\mathbf{y} - \mathbf{x}|}{\varepsilon} \right) w_s d\mathbf{y} .$$

Integrating over  $S$ ,  $\int_S \theta \Phi^0(\Lambda^W \cdot \theta) d\theta = z \Lambda^W$ .  $z$  can be computed using polar coordinates  $\theta = (\cos(s), \sin(s))$  for  $n = 2$  or spherical coordinates  $\theta = (\cos \phi \sin(s), \sin \phi \sin(s), \cos(s))$  for  $n = 3$ , and is given by [15]

$$z = \begin{cases} \int_0^{2\pi} \Phi^0(\cos(s)) \cos(s) ds, & \text{if } n = 2, \\ 2\pi \int_0^\pi \Phi^0(\cos(s)) \cos(s) \sin(s) ds, & \text{if } n = 3. \end{cases} \quad (4.20)$$

We can then write

$$w_f = D\Lambda^W \rho_f - C_f \nabla \rho_f , \quad (4.21)$$

where the alignment and diffusion coefficients are respectively given by

$$D = \frac{z(1-\zeta)}{(1-\zeta\nu_1)} \quad \text{and} \quad C_f = \frac{c_f}{\beta(1-\zeta\nu_1)} .$$

The macroscopic PDE description for the follower population is

$$\partial_t \rho_f + c_f \nabla \cdot (D\Lambda^W \rho_f - C_f \nabla \rho_f) = 0 . \quad (4.22)$$

Finally, the system describing the macroscopic densities of followers and leaders, in the diffusion limit, reads as follows

$$c_s \mathbf{b} \cdot \nabla \rho_s - R_{sp}^0 \rho_s + R_{ps}^0 \rho_p = 0 , \quad (4.23)$$

$$\partial_t \rho_p - nc_p \Delta (D \rho_p) + nc_p \nabla \cdot (\mathcal{R}_{sp}^0 \rho_s) + nc_p R_{ps}^0 \nabla \cdot (\mathcal{B}_\theta^0 \rho_p) = 0 , \quad (4.24)$$

$$\partial_t \rho_f + c_f \nabla \cdot (D\Lambda^W \rho_f - C_f \nabla \rho_f) = 0 . \quad (4.25)$$

## 4.2 Hyperbolic limit

In this section we investigate the dynamics of the swarm over shorter time scales. Consider the following scaling  $(\mathbf{x}, t) \mapsto (\mathbf{x}/\varepsilon, t/\varepsilon)$ , then we write

$$\varepsilon \partial_t \rho_s - \varepsilon c_s \mathbf{b} \cdot \nabla \rho_s = -\varepsilon R_{sp}^\varepsilon \rho_s + \varepsilon R_{ps}^\varepsilon \rho_p , \quad (4.26)$$

$$\varepsilon \partial_t \sigma_p + \varepsilon c_p \theta \cdot \nabla \sigma_p = \varepsilon R_{sp}^\varepsilon(\theta) \rho_s - \varepsilon R_{ps}^\varepsilon \sigma_p - \beta \sigma_p + |S| \beta B^\varepsilon \rho_p , \quad (4.27)$$

$$\varepsilon \partial_t \sigma_f + \varepsilon c_f \theta \cdot \nabla \sigma_f = -\beta \sigma_f + \zeta \beta T \sigma_f + (1-\zeta) \beta \Phi^\varepsilon(\Lambda \cdot \theta) \rho_f . \quad (4.28)$$

The conservation equation (4.6) in this case is given by

$$\varepsilon \partial_t \rho_\ell + \varepsilon n c_p \nabla \cdot w_p - \varepsilon c_s \nabla \cdot (\mathbf{b} \rho_s) = 0 . \quad (4.29)$$

Following the same procedure as before we consider the expansion (4.11) and from (4.27) we obtain

$$\sigma_p^0 = |S| B^0 \rho_p . \quad (4.30)$$

Hence, substituting  $\sigma_p = |S| B^0 \rho_p + \varepsilon \sigma_p^1 + \mathcal{O}(\varepsilon^2)$  into the mean direction  $w_p$ , as defined in (4.5), the conservation equation reads

$$\partial_t (\rho_p + \rho_s) + nc_p \nabla \cdot (\mathcal{B}_\theta^0 \rho_p + \frac{\varepsilon}{|S|} \int_S \theta \sigma_p^1 d\theta) - c_s \nabla \cdot (\mathbf{b} \rho_s) = 0 . \quad (4.31)$$

The next step is to find the term  $\sigma_p^1$ . Substituting the expansion for  $\sigma_p$  back into (4.27) and letting  $\varepsilon \rightarrow 0$  we get

$$-|S|^{-1} \beta \sigma_p^1 = \rho_p \partial_t B^0 + B^0 \partial_t \rho_p + c_p (\theta \cdot \nabla) (B^0 \rho_p) - |S|^{-1} R_{sp}^0(\theta) \rho_s + R_{ps}^0 B^0 \rho_p . \quad (4.32)$$

Substituting  $\partial_t \rho_p$  from the conservation equation (4.31) we obtain

$$\begin{aligned} -|S|^{-1} \beta \sigma_p^1 &= \rho_p \partial_t B^0 + B^0 \left( -\partial_t \rho_s - nc_p \nabla \cdot (\mathcal{B}_\theta^0 \rho_p) + c_s \nabla \cdot (\mathbf{b} \rho_s) \right) \\ &\quad + c_p (\theta \cdot \nabla) (B^0 \rho_p) - |S|^{-1} R_{sp}^0(\theta) \rho_s + R_{ps}^0 B^0 \rho_p . \end{aligned}$$

We note that from (4.26) we can substitute  $-\partial_t \rho_s + c_s \nabla \cdot (\mathbf{b} \rho_s)$  to obtain

$$\begin{aligned} -|S|^{-1} \beta \sigma_p^1 &= -nc_p B^0 \nabla \cdot (\mathcal{B}_\theta^0 \rho_p) + \rho_p \partial_t B^0 + c_p (\theta \cdot \nabla) (B^0 \rho_p) + B^0 |S| R_{sp}^0 \rho_s \\ &\quad - |S|^{-1} R_{sp}^0 (\theta) \rho_s + B^0 (1 - |S|) R_{ps}^0 \rho_p \\ &= c_p B^0 (\theta - n \mathcal{B}_\theta^0) \cdot \nabla \rho_p + c_p (\theta \cdot \nabla B^0 - n B^0 \nabla \cdot \mathcal{B}_\theta^0) \rho_p + \rho_p \partial_t B^0 \\ &\quad + B^0 |S| R_{sp}^0 \rho_s - |S|^{-1} R_{sp}^0 (\theta) \rho_s . \end{aligned} \quad (4.33)$$

Letting

$$q_1 = c_p B^0 (\theta - n \mathcal{B}_\theta^0) , \quad q_2 = c_p (\theta \cdot \nabla B^0 - n B^0 \nabla \cdot \mathcal{B}_\theta^0) + \partial_t B^0 ,$$

we can write

$$\sigma_p^1 = \frac{-|S|}{\beta} (q_1 \cdot \nabla \rho_p + q_2 \rho_p + B^0 |S| R_{sp}^0 \rho_s - |S|^{-1} R_{sp}^0 (\theta) \rho_s) . \quad (4.34)$$

Finally, by substituting  $\sigma_p^1$  back into the conservation equation (4.31), we obtain

$$\partial_t \rho_\ell + nc_p \nabla \cdot (\mathcal{B}_\theta^0 \rho_p) - c_s \nabla \cdot (\mathbf{b} \rho_s) = \varepsilon nc_p [Q_1 \nabla \rho_p - Q_2 \rho_p + (|S| \mathcal{B}_\theta^0 R_{sp}^0 - \mathcal{R}_{sp}^0 (\theta)) \rho_s] , \quad (4.35)$$

where

$$Q_1 = \frac{1}{\beta} \int_S \theta \cdot q_1 d\theta , \quad Q_2 = \frac{-1}{\beta} \int_S \theta q_2 d\theta .$$

Splitting again the leaders' population into  $\rho_p$  and  $\rho_s$  and substituting  $\partial_t \rho_s$  from (4.26) into (4.35) we obtain

$$\begin{aligned} \partial_t \rho_p + nc_p \nabla \cdot (\mathcal{B}_\theta^0 \rho_p) - R_{sp}^0 \rho_s + R_{ps}^0 \rho_p &= \varepsilon nc_p [Q_1 \nabla \rho_p - Q_2 \rho_p \\ &\quad + (|S| \mathcal{B}_\theta^0 R_{sp}^0 - \mathcal{R}_{sp}^0 (\theta)) \rho_s] . \end{aligned} \quad (4.36)$$

For the case of the follower population and using the hyperbolic scaling we can rewrite (4.28) as

$$\partial_t \sigma_f + c_f \theta \cdot \nabla \sigma_f = \frac{\beta}{\varepsilon} (-\sigma_f + \zeta T \sigma_f + (1 - \zeta) \Phi^0(\Lambda \cdot \theta) \rho_f) , \quad (4.37)$$

and, as  $\varepsilon \rightarrow 0$ , we obtain

$$\sigma_f^0 = (\zeta + (1 - \zeta) \Phi^0(\Lambda \cdot \theta)) \rho_f^0 . \quad (4.38)$$

Here we considered only the first eigenvalue of  $T$ , i.e.  $T \sigma_f = \rho_f^0$  as in Appendix A.

Substituting (4.38) into (4.28) and integrating with respect to  $S$  gives

$$\partial_t \rho_f^0 \int_S (\zeta + (1 - \zeta) \Phi^0(\Lambda \cdot \theta)) d\theta + c_f \int_S \theta \cdot \nabla (\zeta + (1 - \zeta) \Phi^0(\Lambda \cdot \theta)) \rho_f^0 d\theta = 0 , \quad (4.39)$$

where the right hand side is zero using the approximation  $T \sigma_f = T_0 \sigma_f$ . In the left hand side we note that  $\int_S \Phi^0(\Lambda \cdot \theta) d\theta = 1$  and, as before,  $\int_S \theta \Phi^0(\Lambda \cdot \theta) d\theta = z \Lambda$  where  $z$  is given by (4.20). Hence the conservation equation for the followers reads

$$\partial_t \rho_f^0 + c_f z (1 - \zeta) \nabla \cdot (\rho_f^0 \Lambda) = 0 . \quad (4.40)$$

Next we need to find the mean direction  $\rho_f^0 \Lambda$ . Following the same analysis as in [15, 19] we substitute the expansion for  $\sigma_f^0$  given in (4.38) into (4.28) and multiply by  $\theta \cdot v$ , where

$v \in \mathbb{R}^n$  is orthogonal to  $\Lambda$ . Integrating over  $S$  then gives

$$\left( \partial_t \int_S \theta \Psi(\theta) \rho_f^0 d\theta + c_f \int_S \theta \cdot \nabla(\Psi(\theta) \rho_f^0) \theta d\theta \right) \cdot v = \mathcal{O}(\varepsilon). \quad (4.41)$$

Here  $\Psi(\theta) = \zeta + (1 - \zeta)\Phi^0(\Lambda \cdot \theta)$ , and letting  $\varepsilon \rightarrow 0$  in the right hand side we obtain

$$\left( z(1 - \zeta) \partial_t(\rho_f^0 \Lambda) + c_f \int_S \theta \cdot \nabla(\rho_f^0 \Psi(\theta)) \theta d\theta \right) \cdot v = 0.$$

Using the fact that  $v \perp \Lambda$ , we can reformulate the above expression in terms of the orthogonal projection  $P_\perp = \mathbb{1} - \Lambda \otimes \Lambda$  onto  $\Lambda^\perp$ ,

$$P_\perp \left( z(1 - \zeta) \partial_t(\rho_f^0 \Lambda) + c_f \nabla \cdot \rho_f^0 \int_S (\theta \otimes \theta) \Psi(\theta) d\theta \right) = 0. \quad (4.42)$$

For the first term of the above expression we can write

$$z(1 - \zeta) P_\perp(\rho_f^0 \partial_t \Lambda + \Lambda \partial_t \rho_f^0) = z(1 - \zeta) \rho_f^0 \partial_t \Lambda, \quad (4.43)$$

since  $\langle \partial_t \Lambda, \Lambda \rangle = \frac{1}{2} \partial_t |\Lambda|^2 = 0$ , i.e.,  $\Lambda \perp \partial_t \Lambda$ . For the second term we must compute the integral  $\int_S (\theta \otimes \theta) \Psi(\theta) d\theta$ , where we use  $\theta = \cos(s)\Lambda + \sin(s)\Lambda^\perp$  in polar coordinates for  $n = 2$  and spherical coordinates for  $n = 3$  as in [15]. Finally, we obtain

$$\rho_f^0 (z(1 - \zeta) \partial_t \Lambda + C_1 \Lambda \cdot \nabla \Lambda) + C_2 P_\perp \nabla \rho_f^0 = 0, \quad (4.44)$$

where we have used  $\Lambda^\perp \otimes \Lambda^\perp = \mathbb{1} - \Lambda \otimes \Lambda$ . Here  $C_1 = c_f(1 - \zeta)a_3$  and  $C_2 = c_f(1 - \zeta)\mathbb{1}a_1 + c_f\mathbb{1}\pi\zeta$  for,  $a_3 = a_0 - a_1$  and

$$a_0 = \begin{cases} \int_0^{2\pi} \Phi^0(\cos(s)) \cos(s)^2 ds, & \text{if } n = 2, \\ 2\pi \int_0^\pi \Phi^0(\cos(s)) \cos(s)^2 \sin(s) ds, & \text{if } n = 3, \end{cases} \quad (4.45)$$

$$a_1 = \begin{cases} \int_0^{2\pi} \Phi^0(\cos(s)) \sin(s)^2 ds, & \text{if } n = 2, \\ \pi \int_0^\pi \Phi^0(\cos(s)) \sin(s)^3 \sin(s) ds, & \text{if } n = 3. \end{cases} \quad (4.46)$$

The final system of equations is given as

$$\partial_t \rho_s - c_s \mathbf{b} \cdot \nabla \rho_s + R_{sp}^0 \rho_s - R_{ps}^0 \rho_p = 0, \quad (4.47)$$

$$\begin{aligned} \partial_t \rho_p + n c_p \nabla \cdot (\mathcal{B}_\theta^0 \rho_p) - R_{sp}^0 \rho_s + R_{ps}^0 \rho_p &= \varepsilon n c_p \left[ Q_1 \nabla \rho_p - Q_2 \rho_p \right. \\ &\quad \left. + \left( |S| \mathcal{B}_\theta^0 R_{sp}^0 - \mathcal{R}_{sp}^0(\theta) \right) \rho_s \right], \end{aligned} \quad (4.48)$$

$$\partial_t \rho_f + c_f z(1 - \zeta) \nabla \cdot (\rho_f \Lambda) = 0, \quad (4.49)$$

$$\rho_f (z(1 - \zeta) \partial_t \Lambda + C_1 \Lambda \cdot \nabla \Lambda) + C_2 P_\perp \nabla \rho_f = 0. \quad (4.50)$$

### 4.3 Discussion of macroscopic equations

The macroscopic equations obtained above capture behaviours depicted in Figures 1 and 2 according to their respective scales. From Equation (4.23), we observe that the distribution of streakers on long (parabolic) time scales is constant along the vector field  $\mathbf{b}$  whenever  $R_{sp}^0$  and  $R_{ps}^0$  vanish, i.e. within the interior of the swarm. At the front of the swarm, the lower bound  $R_{sp}^0 \geq r_0$  forces  $\rho_s$  to decay exponentially fast to zero over

a characteristic length scale  $\frac{c_s}{r_0}$ , as streakers convert to passive leaders. Equation (4.24) reflects an undirected diffusion of the passive leaders through the swarm, with a transport term  $\nabla \cdot (\mathcal{B}_\theta^0 \rho_p)$  corresponding to the velocity opposite those of the streakers. As passive leaders reach areas of large  $R_{ps}^0$ , corresponding to the rear boundary of the swarm, they convert to streakers and head again to the swarm front. The characteristic length scale is  $\frac{c_p}{r_0}$ . Note that the movement of streakers and passive leaders only depends on the followers through the transition rates  $R_{sp}^0$  and  $R_{ps}^0$ : this is logical enough, given that leaders have knowledge of the nest site and should not be swayed by the uninformed. A more detailed model may also incorporate some influence of the followers on the leader direction (e.g. due to avoiding collisions), however we have neglected that here for simplicity.

From (4.25), the density of followers also diffuses over parabolic time scales. The directional movement of the swarm depends on the leaders only through  $\Lambda^W$ . This highlights the limitations of modelling via the homogeneous alignment kernel (3.2): since  $\Lambda^W$  is a unit vector, only a single leader is required to direct the swarm to its nest, a result which clearly stretched credulity for large swarms. This pathology motivates the study of inhomogeneous alignment kernels in Section 5, where the size of the orientation vector  $\Lambda^W$  is taken to increase both with the number of leaders moving along  $\mathbf{b}$  and with the strength of the interactions.

A basic question concerns whether two follower populations, as in Figure 2, behave as one joint swarm or two separate swarms. From previous discussions in Section 3, for the model here the distinction lies with the separation of the two populations: for separations much larger than  $\frac{c_s}{r_0}$ , leaders remain confined to their separate follower swarms; for separations smaller than  $\frac{c_s}{r_0}$ , the leader populations bridge the gap that separates the peaks to join the swarms together; streakers to passive leader conversion occurs predominantly within a single zone at the swarm front.

Equations (4.47) to (4.50) for shorter, hyperbolic time scales support the general description above, with a few notable modifications. First, over this shorter time scale the streakers follow a transport equation (4.47) that includes a time derivative absent from the parabolic limit, allowing a time-dependent description of streaker movement through the swarm. Second, the passive leader distribution in (4.48) does not undergo undirected diffusion over hyperbolic time scales, rather it is simply transported in the opposite direction to the streakers with its respective velocity. The terms of order  $\varepsilon$  account for secondary effects in the collective movement. Finally, the equations for the followers, (4.49) and (4.50), correspond to classical equations for swarming particles [19]. Again, the directional movement of the swarm depends on the leaders only through  $\Lambda^W$ , and the swarm impacts on the movement of the leaders only through the switching rates  $R_{sp}^0$  and  $R_{ps}^0$ .

## 5 Inhomogeneous alignment kernel

In this section we consider the alignment kernel given by

$$\Lambda^* = \nu \mathcal{J}(\mathbf{x}, t) \quad (5.1)$$

where we have removed the normalization and  $\mathcal{J}(\mathbf{x}, t)$  is given as in (3.2). Here we limit our discussion to the case  $n = 2$ . Parameter  $\nu$  is the relaxation frequency, previously

assumed constant but in this approach taken to depend on the norm of  $\mathcal{J}(\mathbf{x}, t)$ . Here we study the diffusion and hyperbolic limit of the system for follower-leader interactions, as previously done in Section 4. In particular, we focus on the equation for followers (4.10) and (4.28) under an alignment given by (5.1).

The distribution of aligned directions  $\Phi(\Lambda^* \cdot \theta)$  in (3.9) is replaced by

$$\bar{\Phi}(\Lambda^* \cdot \theta) = \frac{\Phi(\Lambda^* \cdot \theta)}{\int_0^{2\pi} \Phi(|\Lambda^*| \cos \theta) d\theta} \quad (5.2)$$

such that  $\int_S \bar{\Phi}(\Lambda^* \cdot \theta) d\theta = 1$ .

In the diffusion limit, we replace  $\Phi^0(\Lambda \cdot \theta)$  by  $\bar{\Phi}^0(\Lambda^* \cdot \theta)$  in equations (4.18) and (4.19). Noting that

$$\int_S \theta \bar{\Phi}^0(\Lambda^{*W} \cdot \theta) d\theta = \bar{z} \Lambda^{*W}, \quad \text{where } \bar{z} = |\Lambda^*| \int_0^{2\pi} \bar{\Phi}^0(|\Lambda^*| \cos(s)) \cos(s) ds, \quad (5.3)$$

for  $\theta = \cos(s)\Lambda^* + \sin(s)\Lambda^{*\perp}$  we again obtain (4.22), where in this case

$$D = \frac{\bar{z}(1 - \zeta)}{n(1 - \zeta\nu_1)}.$$

For the hyperbolic limit, let us first define the right hand side of (4.37) as

$$L(\sigma_f) = -\beta\sigma_f + \beta\zeta T\sigma_f + (1 - \zeta)\beta\bar{\Phi}^\varepsilon(\Lambda^* \cdot \theta)\rho_f.$$

We know that as  $\varepsilon \rightarrow 0$  the solution  $\sigma_f^0 = \bar{\Psi}(\theta)\rho_f^0$ , where  $\bar{\Psi}(\theta) = \zeta + (1 - \zeta)\bar{\Phi}^0(\Lambda^* \cdot \theta)$ . The new operator  $\bar{\Psi}(\theta)$  needs to be a Generalized Collisional Invariant of the operator  $L(\sigma_f)$ , as in the following sense [13, 14, 15].

**Definition 5.1** A function  $\bar{\Psi}(\theta)$  is a Generalized Collisional Invariant of  $Q$  if it satisfies

$$\int_S L(\sigma_f) \bar{\Psi}(\theta) d\theta = 0,$$

for any  $\sigma_f$ . Equivalently,  $\sigma_f$  satisfies  $P_\perp \left( \int_S \sigma_f(\mathbf{x}, t, \theta) \theta d\theta \right) = 0$ , where  $P_\perp = \text{Id} - \Lambda^* \otimes \Lambda^*$  is an orthogonal projection to  $\Lambda^*$ .

Note that for the case  $\zeta = 0$ , i.e. when only alignment is considered, from Definition 5.1 we conclude that  $\int_S L(\sigma_f) \bar{\Phi}^0(\Lambda^* \cdot \theta) d\theta = 0$ , where  $\bar{\Phi}^0$  can be taken as the von Mises-Fisher distribution. Then, the analysis in [13] follows. The system (4.49)-(4.50) can be written now as

$$\partial_t \rho_f + c_f \bar{z}(1 - \zeta) \nabla \cdot (\rho_f \Lambda^*) = 0, \quad (5.4)$$

$$\rho_f (\bar{z}(1 - \zeta) \partial_t \Lambda^* + \bar{C}_1 \Lambda^* \cdot \nabla \Lambda^*) + \bar{C}_2 P_\perp \nabla \rho_f = 0, \quad (5.5)$$

where  $\bar{z}$  is given by (5.3) and, similar to previous derivation,  $\bar{C}_1 = c_f(1 - \zeta)\bar{a}_3$ ,  $\bar{C}_2 = c_f(1 - \zeta)\mathbf{1}\bar{a}_1 + c_f\mathbf{1}\pi\zeta$  for,  $\bar{a}_3 = \bar{a}_0 - \bar{a}_1$  with

$$\bar{a}_0 = |\Lambda^*|^2 \int_0^{2\pi} \bar{\Phi}^0(|\Lambda^*| \cos(s)) \cos^2(s) ds, \quad \bar{a}_1 = |\Lambda^*|^2 \int_0^{2\pi} \bar{\Phi}^0(|\Lambda^*| \cos(s)) \sin^2(s) ds.$$

## 6 Discussion

The capacity of individuals to coordinate their movement to generate collective movement is a phenomenon that has attracted significant interest, in both cellular and animal systems. Much of the progress in this area has been facilitated through modelling studies, particularly via the employment of agent-based (or particle) descriptions that consider the movement response of each single member according to its neighbours. Yet the largest swarms can extend over kilometres and contain millions (e.g. herrings, [27]) or even hundreds of billions (e.g. desert locusts, [34, 42]) of members. At such numbers and scales, continuous modelling approaches become necessary for their efficiency and increased tractability. Consequently, there is a clear interest in clarifying the relevant form of continuous models for swarming systems.

Much recent interest has focussed on follower-leader systems, where the population is decomposed into a leader population which somehow guides a population of followers. Honeybee swarms offer an ideal case study for exploring the continuous modelling of follower-leader systems: given their large size ( $O(10^4)$  individuals), a continuous approach is relevant and a significant body of work has elucidated key insights into how the distinct leader population guides the uninformed followers [38]. Inspired by this system we have formulated a minimalistic microscopic description for a population of informed scouts and the followers, deriving the ensuing macroscopic models under distinct scaling limits. To test the extent to which velocity alignment by itself can propel a guided and coherent swarm, follower orientation is limited to the interaction choice (3.3): alignment according to the velocity direction. Under both hyperbolic and parabolic scaling, macroscopic models feature drift-terms with advection in the streaking direction. Thus, alignment to velocity alone yields translocation of the swarm towards the nest.

Under the hyperbolic scaling a pure-drift equation is generated, implying the potential for travelling-pulses with movement of a cohesive colony towards the nest site. The parabolic limit, on the other hand, generates a drift-diffusion equation. While drift is in the direction of the nest site, the additional dispersion leads to swarm spreading with time. Early stretching of the colony is to be expected, as the initially tight cluster morphs into a migrating swarm. Once a swarm is established, however, it appears to retain a relatively stable speed and shape: any continued dispersal would be far from optimal, leading to colony loss (bees losing contact and becoming “lost”) and placing the all-important queen at risk of exposure. Of course, the question of which is the appropriate limit boils down to the relevant spatio-temporal scales. Straight-line motions of follower bees within a swarm is unlikely to be longer than a few seconds or so, longer runs would move them beyond swarm boundaries. At a macroscopic scale, swarms travel from a few hundred metres (over a few minutes) to multiple kilometres (up to an hour) to new nest locations [1]. While the hyperbolic model may be relevant for shorter swarm migrations, over larger migrations the parabolic scaling would be necessary.

The above must be viewed in light of our intentionally simple modelling approach, where we have specifically tested the practicalities of an “alignment-only” mechanism. Agent-based approaches for modelling bee swarms (and, indeed, swarming phenomena in general) are typically augmented by additional attractive/cohesion behaviours, where individuals are also pulled in the direction of those in their neighbourhood; in non-local

continuous models, a similar effect is gained through a nonlocal attraction term that biases movement direction. As stressed above, we have reasonably excluded such considerations from the present model for simplicity, however including nonlocal attractions could clearly counteract swarm dispersal. For example, following [2], attraction (or repulsion) between individuals can be considered by

$$\mathcal{A} = \left( \frac{d_c - \text{dist}(\mathbf{x}, \mathbf{y})}{\text{dist}(\mathbf{x}, \mathbf{y})} \right) e^{-(d_c - \text{dist}(\mathbf{x}, \mathbf{y}))^2} \vec{e}(\mathbf{x}, \mathbf{y}).$$

Here  $\text{dist}(\mathbf{x}, \mathbf{y})$  denotes the distance between two individuals  $\mathbf{x}$  and  $\mathbf{y}$ , along the direction of the unit vector  $\vec{e}(\mathbf{x}, \mathbf{y})$ . If  $\text{dist}(\mathbf{x}, \mathbf{y}) < d_c$ , where  $d_c$  is a critical distance, then the action of  $\mathcal{A}$  is repulsive and if  $\text{dist}(\mathbf{x}, \mathbf{y}) > d_c$  we have attraction.

Recently, there has been considerable interest in the composition and structuring of swarming populations. For example, in the case of bird flocks and fish shoals, the existence of faster and/or braver individuals can lead to hierarchical swarm arrangements [35, 31] and the question is raised as to how much swarm movement is dominated by the choice of a few. For simplicity, the movements of our leaders has been set here somewhat naively: during streaks, they operate as ballistic particles adopting fast movements towards the nest. While this may be a reasonable approximation for bee swarms, where leaders have specific *a priori* knowledge, more general “leaders” may be more subtle and get influenced by neighbour movements. Consequently, a logical extension would be to also adopt a velocity jump model for the leader population, where one of their movement contributions stems from an interaction function similar to (3.3), distinctly weighted. In other instances, leader/follower statuses may be transient, for example resulting from spatial position within the swarm, and it may be necessary to include switching terms between follower and leader populations.

The study of population dynamics, where a few discrete agents act as leaders, provides an excellent scenario to derive specific control laws and interactions that drive self-organisation, leading the swarm optimally to a desired outcome. This will allow an analytic understanding of follower-leader interactions, with applications not only to understanding the collective dynamics of biological populations but also outside biology, for example to hierarchical swarms of robots.

## Appendix A Turn angle operator

This section recalls some basic spectral properties of the turn angle operator  $T$  defined in (3.1). Recall that in  $n$ -dimensions, the surface area of the unit sphere  $S$  is given by

$$|S| = \begin{cases} \frac{2\pi^{n/2}}{\Gamma(\frac{n}{2})}, & \text{for } n \text{ even,} \\ \frac{\pi^{n/2}}{\Gamma(\frac{n}{2}+1)}, & \text{for } n \text{ odd.} \end{cases}$$

**Lemma 1** *Assume that  $\tilde{k}$  is continuous. Then  $T$  is a symmetric compact operator. In particular, there exists an orthonormal basis of  $L^2(S)$  consisting of eigenfunctions of  $T$ .*

With  $\theta = (\theta_0, \theta_1, \dots, \theta_{n-1}) \in S$ , we have

$$\begin{aligned} \phi_0(\theta) &= \frac{1}{|S|} \quad \text{is an eigenfunction to the eigenvalue} \quad \nu_0 = 1, \\ \phi_1^j(\theta) &= \frac{n\theta_j}{|S|} \quad \text{are eigenfunctions to the eigenvalue} \quad \nu_1 = \int_S \tilde{k}(\cdot, |\eta - 1|) \eta_1 d\eta < 1. \end{aligned} \quad (\text{A } 1)$$

Any function  $\sigma \in L^2(\mathbb{R}^n \times \mathbb{R}^+ \times S)$  admits a unique decomposition

$$\sigma(\mathbf{x}, t, \theta) = \frac{1}{|S|} (u + n\theta \cdot w) + \hat{z}, \quad (\text{A } 2)$$

where  $\hat{z}$  is orthogonal to all linear polynomials in  $\theta$ . Explicitly,

$$u(\mathbf{x}, t) = \int_S \sigma(\mathbf{x}, t, \theta) \phi_0(\theta) d\theta, \quad w^j(\mathbf{x}, t) = \int_S \sigma(\mathbf{x}, t, \theta) \phi_1^j(\theta) d\theta,$$

and  $w = (w^1, \dots, w^n)$ .

## References

- [1] Madeleine Beekman, Robert L Fathke, and Thomas D Seeley. How does an informed minority of scouts guide a honeybee swarm as it flies to its new home? *Animal Behaviour*, 71(1):161–171, 2006.
- [2] Nicola Bellomo. *Modeling complex living systems: a kinetic theory and stochastic game approach*. Springer Science & Business Media, 2008.
- [3] Andrew M Berdahl, Albert B Kao, Andrea Flack, Peter AH Westley, Edward A Codling, Iain D Couzin, Anthony I Dell, and Dora Biro. Collective animal navigation and migratory culture: from theoretical models to empirical evidence. *Philosophical Transactions of the Royal Society B: Biological Sciences*, 373(1746):20170009, 2018.
- [4] Sara Bernardi and Annachiara Colombi. A particle model reproducing the effect of a conflicting flight information on the honeybee swarm guidance. *Communications in Applied and Industrial Mathematics*, 9(1):159–173, 2018.
- [5] Sara Bernardi, Annachiara Colombi, and Marco Scianna. A discrete particle model reproducing collective dynamics of a bee swarm. *Computers in biology and medicine*, 93:158–174, 2018.
- [6] Sara Bernardi, Annachiara Colombi, and Marco Scianna. A particle model analysing the behavioural rules underlying the collective flight of a bee swarm towards the new nest. *Journal of Biological Dynamics*, 12(1):632–662, 2018.
- [7] Lauren JN Brent, Daniel W Franks, Emma A Foster, Kenneth C Balcomb, Michael A Cant, and Darren P Croft. Ecological knowledge, leadership, and the evolution of menopause in killer whales. *Current Biology*, 25(6):746–750, 2015.
- [8] José A Carrillo, Massimo Fornasier, Giuseppe Toscani, and Francesco Vecil. Particle, kinetic, and hydrodynamic models of swarming. In *Mathematical Modeling of Collective Behavior in Socio-Economic and Life Sciences*, pages 297–336. Springer, 2010.
- [9] Iain D Couzin, Jens Krause, Nigel R Franks, and Simon A Levin. Effective leadership and decision-making in animal groups on the move. *Nature*, 433(7025):513, 2005.
- [10] Iain D Couzin, Jens Krause, Richard James, Graeme D Ruxton, and Nigel R Franks. Collective memory and spatial sorting in animal groups. *Journal of Theoretical Biology*, 218(1):1–11, 2002.
- [11] Felipe Cucker and Steve Smale. Emergent behavior in flocks. *IEEE Transactions on Automatic Control*, 52(5):852–862, 2007.
- [12] Felipe Cucker and Steve Smale. On the mathematics of emergence. *Japanese Journal of Mathematics*, 2(1):197–227, 2007.

- [13] Pierre Degond, Amic Frouvelle, and Jian-Guo Liu. Macroscopic limits and phase transition in a system of self-propelled particles. *Journal of nonlinear science*, 23(3):427–456, 2013.
- [14] Pierre Degond and Sébastien Motsch. Continuum limit of self-driven particles with orientation interaction. *Mathematical Models and Methods in Applied Sciences*, 18(supp01):1193–1215, 2008.
- [15] Giacomo Dimarco and Sébastien Motsch. Self-alignment driven by jump processes: Macroscopic limit and numerical investigation. *Mathematical Models and Methods in Applied Sciences*, 26(07):1385–1410, 2016.
- [16] Konrad Diwold, Timothy M Schaerf, Mary R Myerscough, Martin Middendorf, and Madeleine Beekman. Deciding on the wing: in-flight decision making and search space sampling in the red dwarf honeybee *apis florea*. *Swarm Intelligence*, 5(2):121–141, 2011.
- [17] R Eftimie, G De Vries, MA Lewis, and F Lutscher. Modeling group formation and activity patterns in self-organizing collectives of individuals. *Bulletin of Mathematical Biology*, 69(5):1537, 2007.
- [18] Raluca Eftimie. Hyperbolic and kinetic models for self-organized biological aggregations and movement: a brief review. *Journal of mathematical biology*, 65(1):35–75, 2012.
- [19] Gissell Estrada-Rodriguez and Heiko Gimperlein. Interacting particles with levy strategies: limits of transport equations for swarm robotic systems. *arXiv preprint arxiv:1807.10124*, 2019.
- [20] RC Fetecau and A Guo. A mathematical model for flight guidance in honeybee swarms. *Bulletin of Mathematical Biology*, 74(11):2600–2621, 2012.
- [21] Uwe Greggers, Caspar Schoening, Jacqueline Degen, and Randolph Menzel. Scouts behave as streakers in honeybee swarms. *Naturwissenschaften*, 100(8):805–809, 2013.
- [22] Anna Haeger, Katarina Wolf, Mirjam M Zegers, and Peter Friedl. Collective cell migration: guidance principles and hierarchies. *Trends in cell biology*, 25(9):556–566, 2015.
- [23] Ali Jadbabaie, Jie Lin, and A Stephen Morse. Coordination of groups of mobile autonomous agents using nearest neighbor rules. *Departmental Papers (ESE)*, page 29, 2003.
- [24] Stefan Janson, Martin Middendorf, and Madeleine Beekman. Honeybee swarms: how do scouts guide a swarm of uninformed bees? *Animal Behaviour*, 70(2):349–358, 2005.
- [25] Tanya Latty, Michael Duncan, and Madeleine Beekman. High bee traffic disrupts transfer of directional information in flying honeybee swarms. *Animal Behaviour*, 78(1):117–121, 2009.
- [26] Martin Lindauer. Schwarmbienen auf wohnungssuche. *Zeitschrift für vergleichende Physiologie*, 37(4):263–324, 1955.
- [27] Nicholas C Makris, Purnima Ratilal, Srinivasan Jagannathan, Zheng Gong, Mark Andrews, Ioannis Bertsatos, Olav Rune Godø, Redwood W Nero, and J Michael Jech. Critical population density triggers rapid formation of vast oceanic fish shoals. *Science*, 323(5922):1734–1737, 2009.
- [28] Roberto Mayor and Sandrine Etienne-Manneville. The front and rear of collective cell migration. *Nature reviews Molecular cell biology*, 17(2):97, 2016.
- [29] Alexander Mogilner and Leah Edelstein-Keshet. A non-local model for a swarm. *Journal of Mathematical Biology*, 38(6):534–570, 1999.
- [30] Thomas Mueller, Robert B OHara, Sarah J Converse, Richard P Urbanek, and William F Fagan. Social learning of migratory performance. *Science*, 341(6149):999–1002, 2013.
- [31] Máté Nagy, Zsuzsa Akos, Dora Biro, and Tamás Vicsek. Hierarchical group dynamics in pigeon flocks. *Nature*, 464(7290):890, 2010.
- [32] Hans G Othmer, Steven R Dunbar, and Wolfgang Alt. Models of dispersal in biological systems. *Journal of mathematical biology*, 26(3):263–298, 1988.
- [33] KJ Painter, JM Bloomfield, JA Sherratt, and A Gerisch. A nonlocal model for contact attraction and repulsion in heterogeneous cell populations. *Bulletin of mathematical biology*, 77(6):1132–1165, 2015.
- [34] RC Rainey. Radar observations of locust swarms. *Science*, 157(3784):98–99, 1967.

- [35] Stephan G Reefs. Can a minority of informed leaders determine the foraging movements of a fish shoal? *Animal behaviour*, 59(2):403–409, 2000.
- [36] Elisa Rigosi, Steven D Wiederman, and David C O’Carroll. Visual acuity of the honey bee retina and the limits for feature detection. *Scientific reports*, 7:45972, 2017.
- [37] Kevin M Schultz, Kevin M Passino, and Thomas D Seeley. The mechanism of flight guidance in honeybee swarms: subtle guides or streaker bees? *Journal of Experimental Biology*, 211(20):3287–3295, 2008.
- [38] Thomas D Seeley. *Honeybee democracy*. Princeton University Press, 2010.
- [39] Thomas D Seeley and Susannah C Buhrman. Group decision making in swarms of honey bees. *Behavioral Ecology and Sociobiology*, 45(1):19–31, 1999.
- [40] Thomas D Seeley, Roger A Morse, and P Kirk Visscher. The natural history of the flight of honey bee swarms. *Psyche: A Journal of Entomology*, 86(2-3):103–113, 1979.
- [41] Jackie Shen. Cucker–smale flocking under hierarchical leadership. *SIAM Journal on Applied Mathematics*, 68(3):694–719, 2007.
- [42] R Skaf, GB Popov, and J Roffey. The desert locust: an international challenge. *Philosophical Transactions of the Royal Society of London. B, Biological Sciences*, 328(1251):525–538, 1990.
- [43] Chad M Topaz, Andrea L Bertozzi, and Mark A Lewis. A nonlocal continuum model for biological aggregation. *Bulletin of mathematical biology*, 68(7):1601, 2006.
- [44] Tamás Vicsek, András Czirók, Eshel Ben-Jacob, Inon Cohen, and Ofer Shochet. Novel type of phase transition in a system of self-driven particles. *Physical review letters*, 75(6):1226, 1995.